

# Control for Multi-subsystem Synchronization with Invariant Local Natural Dynamics

Joono Cheong and Chano Kim

**Abstract**—This paper proposes a generalized version of control strategy that enables state synchronization among distributed subsystems without altering the natural dynamics that each separate system is supposed to show. To handle the general case of  $N$ -subsystem with heterogeneous dynamics, a method of dynamic scaling and ring type network topology are proposed. The associated stability bound is analyzed. We performed several experiments to show the validity of stability analysis and dynamic scaling.

## I. INTRODUCTION

The problem of synchronization between networked distributed systems has been an issue for a long time. Among numerous examples, the teleoperation may be the most well-known application that requires synchronization [1]–[3]. Others may be found in various mechanical uniform control [4], shared haptics control [5], and synchronization of car distance in the highway platoon.

The synchronization, among distributed subsystems, cannot be an easy problem because of communication delay in between the connected subsystems. Conventionally in the teleoperation research area, the scattering theory and wave transformation method [1], [6] were prominent strategies to deal with time delay. The problem is that these approaches are so conservative that desired performance may not be met. Recent technologies like  $\mu$ -synthesis and robust control theory [7] could improve the control performance but requires a tremendous amount of mathematical computation.

In reference [8], a new type of synchronization method was proposed, enabling two simultaneous objectives: (i) to synchronize states between the sites and (ii) to preserve natural dynamics in every local subsystem. The property of local invariant dynamics, or objective (ii) in the above, would look strange at first sight because in common sense the synchronization feedback is supposed to alter the natural dynamics. However, the special setting of control structure that creates pole/zero cancelation of induced dynamics enabled us to preserve the natural local dynamics. This property can be utilized in shared haptics with physics simulation [9], where a local input acting on a site must produce the same state change in every other participating site, while the input/output dynamic behavior at each site must be invariant.

This research was supported by the New Growth Engine of Korea Project from the Ministry of Commerce, Industry and Energy (MOCIE).

J. Cheong is with Faculty of Dept. of Control & Instrumentation Eng., Korea University, 208 Seochang-dong, Jochiwon 339-700, S. KOREA jncheong@korea.ac.kr

C. Kim is with the Dept. of Control & Instrumentation Eng., Korea University, 208 Seochang-dong, Jochiwon 339-700, S. KOREA kco1557@korea.ac.kr

Another possible use is in multi-master teleoperation, where an action at any master, for controlling the slave, should be propagated to rest of the masters so that they get to recognize someone else is taking control, while the active user should not feel the dynamic effect coupled from others. We may find various potential applications that the synchronization method could be used for.

This paper is a continuation work of [8], generalizing the synchronization algorithm to include the cases of arbitrary number of heterogeneous distributed subsystems. The rest of the paper is organized as follows. Section II addresses the preliminary for synchronization control, section III generalizes the theory, and section IV presents experimental results; finally section V makes concluding remarks.

## II. SYNCHRONIZATION WITH INVARIANT LOCAL NATURAL DYNAMICS

### A. Synchronization control

Often distributed multiple subsystems are needed to behave in a synchronized way. Among various situations, consider a distributed system with two identical subsystems, each being modeled a mass with damping as follows:

$$\begin{aligned} \text{site 1 : } m\ddot{x}_1(t) + b\dot{x}_1(t) &= f_1(t) + f_2(t - T_2) \\ \text{site 2 : } m\ddot{x}_2(t) + b\dot{x}_2(t) &= f_1(t - T_1) + f_2(t), \end{aligned} \quad (1)$$

where  $m$  and  $b$  are mass and damping coefficient of the systems;  $x_1(t)$  and  $x_2(t)$  denote positions of the subsystems in sites 1 and 2, respectively; and  $f_1(t)$  and  $f_2(t)$  are input forces acting on sites 1 and 2, respectively. Implicitly we assume information of input force is shared on each site through communication network with constant time delays  $T_1$  and  $T_2$ , representing unidirectional delays from site 1 to site 2 and from site 2 to site 1, respectively. Although simple, the distributed system in Eq.(1) has an interesting property that enables synchronization. For bounded and transient  $f_1(t)$  and  $f_2(t)$ , de-synchronization  $e(t) = x_1(t) - x_2(t)$ , in the steady state, becomes zero as long as  $b$  is nonzero, as analyzed in the following.

$$\begin{aligned} \lim_{s \rightarrow 0} sE(s) &= s(X_1(s) - X_2(s)) \\ &= s \frac{1 - e^{-sT_2}}{ms^2 + bs} F_1(s) - s \frac{1 - e^{-sT_1}}{ms^2 + bs} F_2(s) = 0. \end{aligned} \quad (2)$$

Thus, for the cases with only intermittent input, the synchronization can be done only by the natural damping. Even for step input the de-synchronization error is up to a finite amount.

We need to note, however, that such a result is guaranteed only if a sequence of input information, or force in this case,

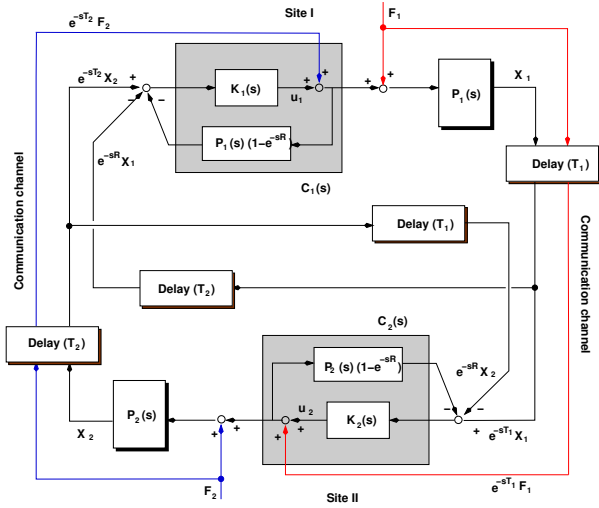


Fig. 1. Proposed synchronization control for identical two subsystems

is accurately conveyed between the two sites with exactly the same initial states. Unfortunately practical network communication possesses many sources of data loss and packet dropout due to unreliability of network and link mechanism. Furthermore, the initial states of the two sites may not be the same. So, to overcome the vulnerability of the open loop distributed systems, we devise a feedback scheme, as shown in Fig.1, which does not deform the natural dynamics and its synchronization characteristics.

*B. Property of invariant local dynamics*

We consider, for the time being, two connected subsystems having the same plant dynamics,  $P_i(s) = P(s), i = 1, 2$  in Fig.1. The round trip delay,  $R$ , is the sum of unilateral delays, that is,  $R = T_1 + T_2$ . The controller,  $C_i(s)$ , consists of linear compensator,  $K_i(s)$ , and state estimator,  $P_i(s)(1 - e^{-sR})$ . Then two algebraic equations from the structure are obtained as:

$$\begin{aligned}
 u_i(s) &= K_i(s) (X_j(s)e^{-sT_j} - X_i(s)e^{-sR}) - \\
 &\quad K_i(s)P_i(s) (1 - e^{-sR}) (u_i(s) + F_j(s)e^{-sT_j}) \quad (3) \\
 X_i(s) &= P(s) (u_i(s) + F_j(s)e^{-sT_j} + F_i(s)) \quad (4)
 \end{aligned}$$

for  $i, j = 1, 2$ , and  $i \neq j$ . Also suppose the case of identical compensators such that  $K_1(s) = K_2(s) = K(s)$ . Then, combining (3) and (4) with simple matrix algebra yields

$$\begin{bmatrix} X_1 \\ X_2 \end{bmatrix} = \begin{bmatrix} P(s) & P(s)e^{-sT_2} \\ P(s)e^{-sT_1} & P(s) \end{bmatrix} \begin{bmatrix} F_1 \\ F_2 \end{bmatrix}. \quad (5)$$

As can be seen, it is exactly a matrix expression in the Laplace variable of open loop natural dynamics in (1). Even under the action of feedback control, the apparent input-output dynamics is still preserved perfectly. This characteristic, that is, the ability to synchronize without altering the local natural dynamics, is the consequence of poles/zeros cancelation occurring in the course of derivation. The can-

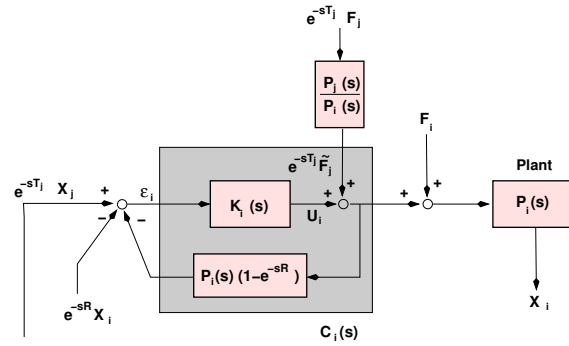


Fig. 2. Input scaling at the  $i$ -th subsystem ( $i \neq j, i, j = 1, 2$ ).

celed part is

$$\begin{aligned}
 \Phi(s) &\triangleq \alpha(s) + \beta(s)e^{-sR} \\
 &= \{P^{-1}(s) + K(s)\}^2 - K^2(s)e^{-sR}, \quad (6)
 \end{aligned}$$

which determines the transient characteristic when there is some source of network disturbance. This characteristic function is a well-known form in the class of linear systems with time delay, and rigorous stability analysis can be found in references such as [10], [11]. Under the assumption that  $\deg[\alpha(s)] > \deg[\beta(s)]$ , the so-called retarded type, and that  $\Phi(s)$  is stable for  $R = 0$ , the following theorem is satisfied.

**Theorem 1. [5]** For the canceled factor in (6),  $\exists$  a constant  $R_{MAD} > 0$ , which is a function of parameters in  $P(s)$  and  $K(s)$  such that the closed loop system has bounded stability if  $0 < R \leq R_{MAD}$ , and (ii) state difference  $|x_1 - x_2| \rightarrow 0$  as  $t \rightarrow \infty$  if  $f_1(t)$  and  $f_2(s)$  are transient and  $b$  is nonzero. ■

For a specific case of  $P(s) = 1/(ms^2 + bs)$  and  $K(s) = k_p + k_v s$ , if  $\bar{b}$  and  $\bar{k}_v/\bar{k}_p$  are much smaller than unity,  $R_{MAD}$ , the maximal allowable delay, can be concisely obtained by following the procedures described in [10] as

$$\begin{aligned}
 R_{MAD} &= \min_l \left( 2l\pi + 4 \tan^{-1} \left( \bar{k}_v \sqrt{2/\bar{k}_p} \right) \right) / \sqrt{2\bar{k}_p} > 0, \\
 l &= \dots, -2, -1, 0, 1, 2 \dots
 \end{aligned}$$

This defines the stability limit of the proposed feedback system.

III. GENERALIZATION

A. Scaling for non-identical subsystems

There are much more cases when distributed subsystems are not identical contrary to the assumption in section II. Then obviously some adjustment of the amounts of input forces must be made, so that the synchronization is smoothly done with a dynamically consistent manner.

For a system with two non-identical subsystems, the natural input/output relation is given as

$$\begin{aligned}
 X_1(s) &= P_1(s) \left( F_1(s) + e^{-sT_2} \tilde{F}_2(s) \right) \\
 X_2(s) &= P_2(s) \left( e^{-sT_1} \tilde{F}_1(s) + F_2(s) \right), \quad (7)
 \end{aligned}$$

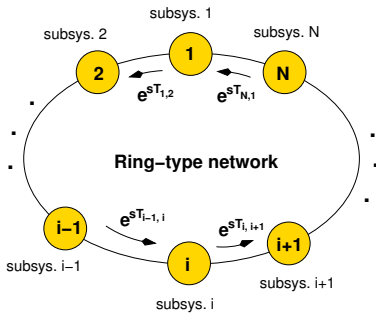


Fig. 3. Network topology of a synchronization control with generic N-subsystem

where  $\tilde{F}_i(s), i = 1, 2$  is the scaled force input compactly defined by

$$\tilde{F}_i(s) = \frac{P_i(s)}{P_j(s)} F_j(s), \quad i \neq j, \text{ and } i, j = 1, 2.$$

The scaling can be interpreted as two successive parts: (i)  $P_i(s)F_i(s)$  produces output, a similar quantity as  $X_i(s)$ , from  $F_i(s)$  only and then (ii) division by  $P_j(s)$  to the output turns it back to input force, but dynamically scaled consistently to the  $j$ -th subsystem. That  $P_i(s)/P_j(s)$  is implementable is the only requirement which makes the scaling possible. And it is only when  $P_i(s)/P_j(s)$  is a proper system where both numerator and denominator polynomials are of the same degree.

The control structure in this case is largely the same as that of the identical subsystems except that each controller must have the corresponding local controller and plant model as shown in Fig.2. With this, we can easily find out that the apparent closed loop input-output relation becomes exactly the same as the open loop relation in Eq.(7). The canceled characteristic function, in this case, that determines the transient behavior is

$$\Phi(s) = (P_1^{-1} + K_1(s))(P_2^{-1} + K_2(s)) - K_1(s)K_2(s)e^{-sR}. \quad (8)$$

Compared to the case with identical subsystems in (6), the above  $\Phi(s)$  is more complicated, and thus to obtain closed-form solution of the corresponding  $R_{MAD}$  is nearly impossible. Practically only numerical solution is available.

### B. Generalization to N-subsystem case

The control principle can be extended to a generic case with N-participating subsystems connected to a ring-type network topology as shown in Fig.3. Data packets are circulating all the way through a closed network, collecting and conveying necessary information. The data communication here is followed by an ordered manner sequentially.

The natural input-output response under this setting is:

$$X_i(s) = P_i(s) \left( \sum_{j=1}^N e^{-sT_{ji}} \frac{P_j(s)}{P_i(s)} F_j(s) \right), \quad i = 1, \dots, N, \quad (9)$$

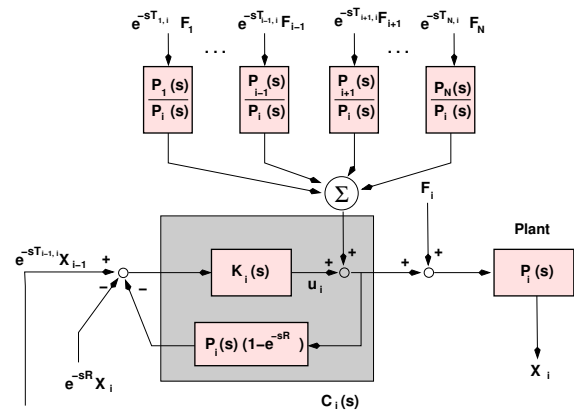


Fig. 4. Controller at the  $i$ -th subsystem

where  $T_{ji}$  denotes the amount of time delay from the  $j$ -th subsystem to the  $i$ -th subsystem, so for  $i = j, T_{ji} = 0$ . The round trip delay,  $R$ , in this case implies the total time that is taken for a data packet to travel the entire ring network completely. At the  $i$ -th subsystem, all the forces at the rest of the subsystems are collected and applied after being scaled dynamically. On top of this open loop setting, we create a controller similar to the previous one as shown in Fig.4. The  $i$ -th subsystem receives output of the  $(i - 1)$ -th subsystem and sends its own output to the  $(i + 1)$ -th subsystem, so that the entire system continuously propagates output of the participating subsystems. By doing so, each subsystem preserves its prescribed input-output relation in Eq.(9) without being affected by combining others. This can be easily verified through similarly applying procedures in (4) – (5).

From the point of the transient behavior which determines the synchronization capability in the presence of disturbances, how many subsystems are connected does really matter. That is, the characteristic function of this generic case is obtained as

$$\Phi(s) = \prod_{i=1}^N (P_i^{-1}(s) + K_i(s)) - e^{-sR} \prod_{i=1}^N K_i(s), \quad (10)$$

where  $\prod$  denotes product operator. The above  $\Phi(s)$  is the most general form of characteristic function that may be imagined in the present problem. Still the form of Eq.(10) is of the retarded type, and claims in Theorem 1 are applicable as well. But, different from the previous two-subsystem example, where all roots are stable for  $R = 0$  under PD control,  $K(s) = k_v s + k_p$ , however, some roots of  $\Phi(s)$  in (10) can possibly have unstable roots for zero delay, even under the same PD control. This is demonstrated in the below for  $N = 3$ . Because the purpose here is to stabilize any unwanted transient behavior, unstable cases will be left out of the present discussion. Conveniently we regard  $R_{MAD}$  of those cases as zero, meaning zero tolerance of time delay.

For an illustration, consider a case where three identical subsystems with  $P(s) = 1/(ms^2 + bs)$  are connected in the synchronization network. The proposed control structure

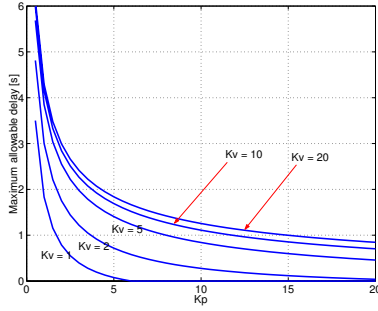


Fig. 5. Numerical values of  $R_{MAD}$ : the case of three identical subsystems.

with  $K(s) = k_p + k_v s$  yields the characteristic function:

$$\Phi(s) = \{P^{-1}(s) + K(s)\}^3 - K^3(s)e^{-sR} .$$

While  $R_{MAD}$  is determined, in general, only by a numerical way, an easy estimate of  $R_{MAD}$  in a closed form is possible by assuming  $\bar{b}$  and  $\bar{k}_v$  are much smaller than  $\bar{k}_p$  as we did previously. That is, the corresponding maximum allowable delay is determined as

$$R_{MAD} = \frac{1}{\sqrt{2\bar{k}_p}} \min_l \left[ (2l + 1)\pi + 6 \tan^{-1} \left( \bar{k}_v \sqrt{\frac{2}{\bar{k}_p}} \right) \right] > 0,$$

where  $l$  is any integer. Fig.5 demonstrates the numerical result of the maximum allowable delay. From the results of the two previous examples, we can generalize that the maximum allowable delay for a distributed system with  $N$  identical subsystems is determined as

$$R_{MAD} = \frac{1}{\sqrt{2\bar{k}_p}} \min_l \left[ \left( 2l + \frac{1 + (-1)^{N+1}}{2} \right) \pi + 2N \tan^{-1} \left( \bar{k}_v \sqrt{\frac{2}{\bar{k}_p}} \right) \right] > 0, \quad (11)$$

where  $l$  is any integer.

#### IV. EXPERIMENTAL STUDY

We verify the stability and performance analyses of the proposed motion control scheme through experimental results. We used one physical robotic system and one virtual system generated in a computer station, each being connected via LAN, exchanging force and state information. The physical system is a one-link robotic master arm driven by direct drive motor and equipped with force sensor at the the gripper as shown in Fig.6.

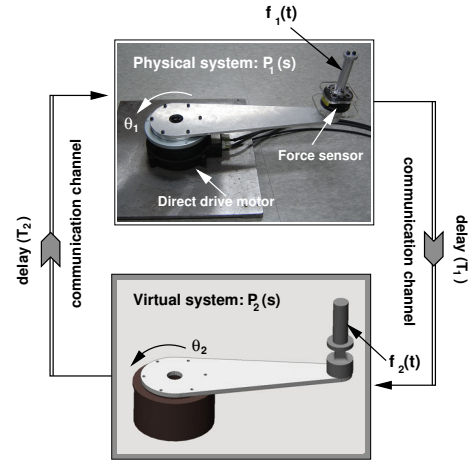


Fig. 6. Experimental setup

Since the dynamics of the physical system must be fully known, thereby for the proposed idea to be implemented in the manner we described, we canceled all the uncertainties in the system after estimating them through disturbance observer (DOB) technique [12]. The nominal dynamic equation of the physical robotic arm is:

$$J_n \ddot{\theta} + b_n \dot{\theta} = l_a f_h, \quad (12)$$

where  $J_n$ ,  $b_n$ , and  $\theta$  denote nominal inertia, nominal damping coefficient, and joint angle, respectively, and also  $l_a$  and  $f_h$  represent robotic arm length and applied force at the gripper by human. Numerical values of all the necessary parameters are summarized in Table I.

The first experimental test was to verify the stability analysis in Theorem 1 and 2. To this end, for various values of  $R$ , we compared output responses of a controlled system having two connected subsystems shown in Fig.6. The dynamics of the virtual subsystem was chosen to be the same as that of the nominal model in (12) of physical counterpart. That is,

$$P_1(s) = P_2(s) = \frac{1}{0.1148s^2 + 0.1912s}.$$

For convenience,  $P_1(s)$  means the physical system, and  $P_2(s)$  is the virtual system in this section, hereafter, without further notice. We assumed two unilateral time delays are equal such that  $T_1 = T_2$ . For the synchronization, we basically adopted the control structure shown in Fig.1 with the following control gains

$$k_p = 10, \quad k_v = 1, \quad (13)$$

which corresponds to 339ms of  $R_{MAD}$ . The input applied for the test was a simple sine wave at site 1 as  $f_1(t) = \sin(2\pi t)$ , but no force at site 2 as  $f_2(t) = 0$ . For three delay conditions, that is,  $R=200$ ms,  $R=300$ ms,  $R=360$ ms, corresponding responses and the created control torque are illustrated in Fig.7. As expected from Theorem 1, the system was stable for the first two delay conditions, where  $R$  was smaller than  $R_{MAD}$ . On the other hand the case of  $R=360$ ms, which is over

TABLE I  
PARAMETERS OF THE ROBOTIC MASTER ARM

contents	value	units
Length of arm ( $l_a$ )	0.45	[m]
Inertia ( $J_n$ )	0.1141	[kg · m <sup>2</sup> ]
Damping coeff. ( $b_n$ )	0.1912	[Nm/s]
Max. torque	30.0	[Nm]
Max. speed	1.7	[rps]

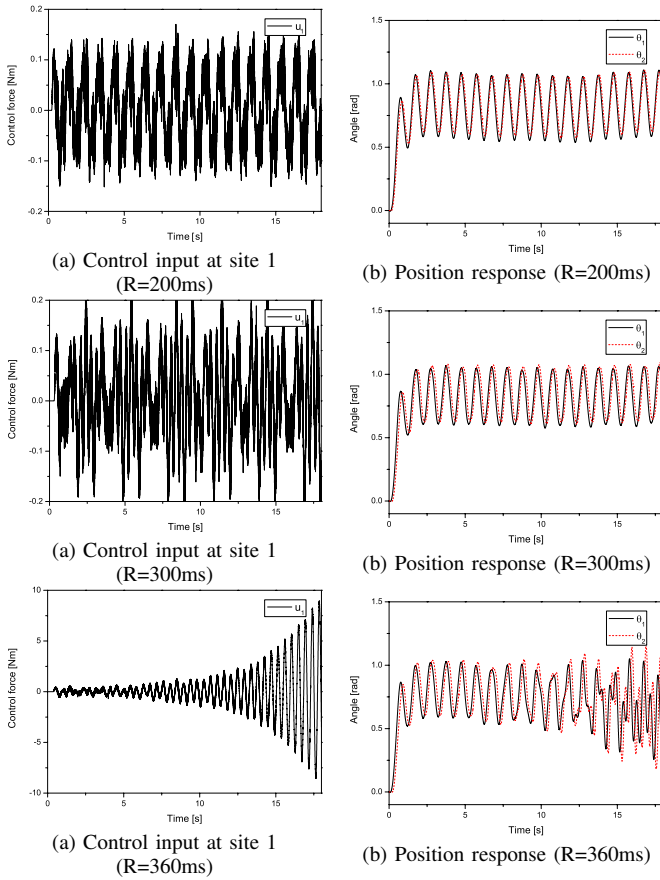


Fig. 7. Responses from sinusoidal input for various time delay

$R_{MAD}$  showed an unstable response. This supports the validity of the stability condition for the proposed scheme, in terms of  $R_{MAD}$ .

Next experiment is to test the effect of dynamic scaling, where we considered that subsystems have different dynamic parameters. To this end, we varied the parameters of the virtual subsystem to

$$P_2(s) = \frac{1}{0.3444s^2 + 0.3824s},$$

by tripling inertia and doubling damping coefficient from the original. Then we observed the controlled responses of the cases with and without dynamic scaling. The only input was human operator's force on the physical master arm, while the output was the positions of the two subsystems. Since time delay did not play an important role in this test, we set  $R = 14ms$ , which is relatively small. During human's back-and-forth motion, approximately one radian amount in angle, holding the gripper of the arm, the synchronization capability degraded so much without dynamic scaling as shown in Fig.8(b). On the contrary, if the dynamic scaling was applied, the synchronization capability was perfectly maintained, for the similar back-and-forth motion. Comparing the force reactions in Fig.8(a) and Fig.8(c), we notice that the human operator, for the case without dynamic scaling, felt approximately two times larger inertial force than for the case with dynamic scaling. This is because some dynamic

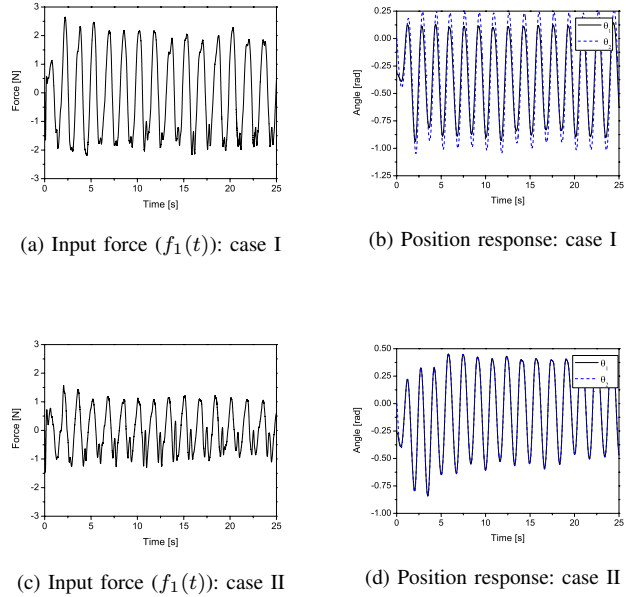


Fig. 8. Experimental results (case I: not scaled; case II: dynamic scaling)

coupling among the connected subsystems exists without dynamic coupling. From the fact that the absolute amount of reaction force with dynamic scaling was almost equal to the same level as the master was operated alone, it is evident that dynamic scaling is needed to preserve the property of local invariant dynamics for subsystems with different dynamic parameters.

Finally we show a possibility to utilize the proposed scheme to teleoperator control. Though the present form of the proposed method may not perfectly match the requirements of cutting edged teleoperator control, it may simply be utilized, in its current form, to common position-position matching teleoperation. And by augmenting much more sophisticated idea like shared control strategy [13], the practical values of the proposed method can be outreached to higher-end teleoperations. The master was the physical robotic arm, and a virtual system with identical dynamics was the slave system. In the slave side placed, at  $\theta = 0.5[rad]$ , was an imaginary stiff wall that produces repulsive force during contact, modeled as

$$f_w := -k_1\delta - k_2\dot{\delta},$$

where  $\delta$  is the penetration distance to wall, and  $k_1$  and  $k_2$  are constant, depending upon material properties. We chose  $(k_1, k_2) = (2000[N/m], 2.5[Ns/m])$ . Explicitly rewriting the effective equations of master/slave teleoperator system gives

$$\begin{aligned} \text{Master : } & J_n \ddot{\theta}_1(t) + b_n \dot{\theta}_1(t) = l_a f_h(t) - l_a f_w(t - T_2) \\ \text{Slave : } & J_n \ddot{\theta}_2(t) + b_n \dot{\theta}_2(t) = l_a f_h(t - T_1) - l_a f_w(t), \end{aligned} \quad (14)$$

where two external forces,  $f_h(t)$  and  $f_w(t)$ , imply local forces at master and slave side, respectively. Certainly we can see the analogy between Eqs. (14) and (1).



While activating the synchronization scheme with the same control parameters in (13), we carried out teleoperation tests moving the master system forward and resisting the wall force reflected backward from the slave side. As shown in Fig.9, in the free motion phase, position synchronization was almost perfectly achieved. However, in the contact phase, we see a somewhat complicated behavior. As the contact began, transient responses appeared and died out for the cases of  $R = 10\text{ms}$  and  $R = 50\text{ms}$ , but on the contrary, the contact transient of the case of  $R = 100\text{ms}$  did not stop and everlasting oscillation was observed. Even for the case of  $R = 50\text{ms}$ , the transient period after contact seemed to be continued a bit longer. The reason is absolutely due to the lack of local feedback for force suppression in the slave side, which the conventional teleoperator controllers have. Thus, a direct force to force interaction occurred between master operator and environment in the slave. The problem in this situation was that timing of human operator's reaction and reflective force from environment may be out of phase as the time delay becomes large. Actually for the case of  $R = 100\text{ms}$  the oscillation frequency by mismatch of force interaction was exactly the reciprocal of a half of  $R$ . A possible remedy toward fixing oscillatory force interaction, without changing the main framework of this scheme, could be to augment a shared strategy which allows some intelligence to slave system to locally manage contact situations in a stable manner [13].

## V. CONCLUSION

This paper presented a new type of motion control scheme for synchronization of distributed subsystems allowing the property of invariant local dynamics of each subsystem. We illustrated the working principle of the control structure for the case of two identical subsystems and then extended the idea to a general case of  $N$  heterogeneous subsystems. In order to deal with the situation having different dynamics among the subsystems, dynamic scaling was applied, and we showed that the property of local invariant dynamics is still preserved. Experimental study confirmed the validity of the claims including stability margin and dynamic scaling. A basic wall contact task along the framework of teleoperation was done and evaluated. Observing the results, we found the proposed scheme was good for position synchronization, but the tasks like wall interaction may need additional treatment for more stable operation.

## REFERENCES

- [1] R. J. Anderson and M. W. Spong, "Bilateral control of teleoperators with time delay," *IEEE Trans. on Automatic Control*, vol. 34, no. 5, pp. 494–501, 1989.
- [2] R. W. Daniel and P. R. McAree, "Fundamental limits of performance for force reflecting teleoperation," *Int. Journ. of Robotics Research*, vol. 17, pp. 811–830, 1998.
- [3] D. A. Lawrence, "Stability and transparency in bilateral teleoperation," *IEEE Trans. on Robotics and Automation*, vol. 9, pp. 624–637, 1993.
- [4] H. H. T. Liu and D. Sun, "Uniform synchronization in multi-axis motion control," in *Proc. of American Control Conference*, pp. 4537–4542, 2005.

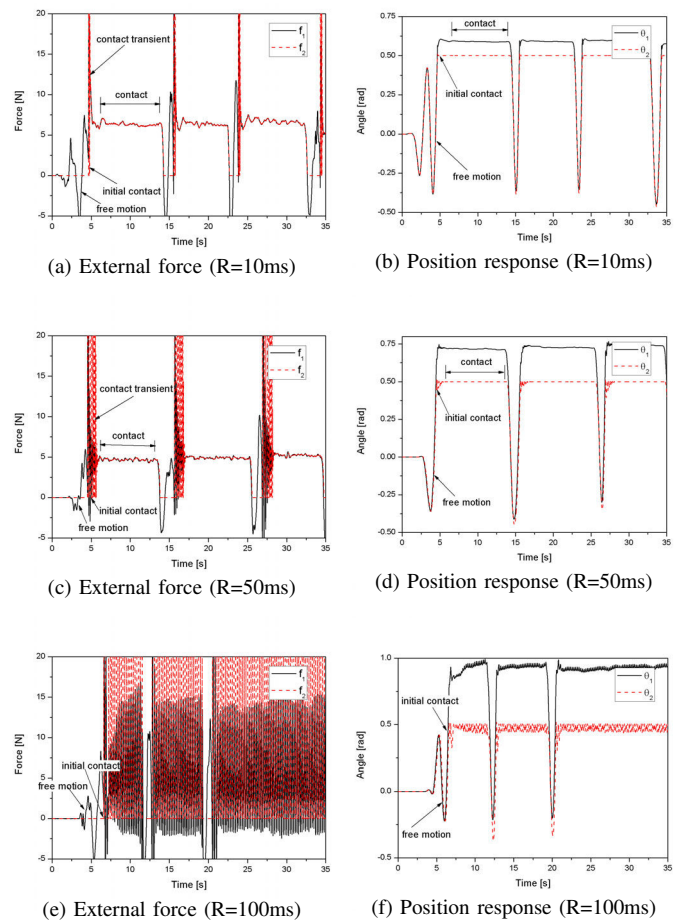


Fig. 9. Teleoperation like experimentation (case I:  $R = 10\text{ms}$ ; case II:  $R = 50\text{ms}$ ; and case II:  $R = 100\text{ms}$ )

- [5] J. Cheong, S.-I. Niculescu, A. Annaswamy, and M. A. Srinivasan, "Motion synchronization in virtual environments with shared haptics and large time delays," in *Proc. of Symp. on Haptic Interfaces for Virtual Environment and Teleoperator Systems*, pp. 277–282, 2005.
- [6] G. Niemeyer and J.-J. E. Slotine, "Stable adaptive teleoperation," *IEEE Journal of Oceanic Engineering*, vol. 16, no. 1, pp. 152–162, 1991.
- [7] J. Yan and S. Salcudean, "Teleoperation controller design using infinity - optimization with application to motion-scaling," *IEEE Trans. on Control System Technologies*, vol. 45, pp. 244–258, 1996.
- [8] J. Cheong, S. Lee, and J. Kim, "Motion duplication control for coupled dynamic systems by natural damping," in *Proc. of IEEE Int. Conf. on Robotics and Automation*, pp. 387–392, 2006.
- [9] J. M. Linebarger and G. D. Kessler, "Concurrency control mechanisms for closely coupled collaboration virtual environments," *Presence*, vol. 13, no. 3, pp. 296–314, 2004.
- [10] K. Walton and J. E. Marshall, "Direct method for tds stability analysis," *IEE Proceedings: Part D*, vol. 2, no. 2, pp. 101–107, 1987.
- [11] S.-I. Niculescu, *Delay Effects on Stability : A Robust Control Approach*. Springer, 2001.
- [12] M. Nakao, K. Ohnishi, and K. Miyachi, "A robust decentralized joint control based on interference estimation," in *Proc. of IEEE Int. Conf. on Robotics and Automation*, pp. 326–331, 1987.
- [13] S. Hayati and S. T. Venkataraman, "Design and implementation of a robot control system with traded and shared control capability," in *Proc. of IEEE Int. Conf. on Robotics and Automation*, pp. 1310–1315, 1989.